An ARM-Enhanced Analysis of GOES-10 Cloud Optical Property Retrievals

S. D. Miller
Naval Research Laboratory
Monterey, California

G. L. Stephens and R. T. Austin
Colorado State University
Ft. Collins, Colorado

Introduction

The vertical variation of cloud microphysical properties (e.g., droplet size distribution, total number concentration, phase, habit) complicates the interpretation of multi-spectral cloud reflection and emission as measured by passive radiometers in space. Solar reflection-based retrievals of cloud optical properties from sensors such as the Geostationary Operational Environmental Satellite (GOES) Imager are based predominantly on a single-layer, plane-parallel assumption (i.e., vertically and horizontally homogeneous) with a single particle size distribution both for computational simplicity and the constraints of the observing system itself. While the particular properties retrieved under these assumptions may yield radiative equivalence for measured cloud top spectral flux, the liquid/ice water paths derived from them can be in significant error owing to a misrepresentation of the true liquid/ice water profile. Feeding these erroneous representations into general circulation models, in turn, will only confuse further the issue of clouds and their role in the current and future climate.

This study explored ways in which active sensors (in particular, the National Aeronautics and Space Administration/Jet Propulsion Laboratory Airborne Cloud Radar [ACR] and the Atmospheric Radiation Measurement [ARM] Program Cloud Detection Lidar [CDL]) and in situ instrumentation (here, the Forward Scattering Spectral Probe [FSSP]) help to shed light on the information content of GOES-10 (135-W) retrievals of cloud optical depth (τ) and effective particle radius (r_e). These parameters are linked intimately to the radiative behavior of clouds via their association with vertically integrated cloud liquid water content. Two ARM-supported field experiments, outlined below, demonstrate this utility in the context of marine stratocumulus and tropical cirrus clouds. The results emphasize the vertical variation of real-world clouds in glaring contrast to the vertically homogenous assumptions invoked by most satellite retrieval methods.

Retrieval Background

The cloud retrievals of this study were based on a maximum likelihood estimation method following directly from Rodgers (1976) and applied to satellite radiometer data by Miller et al. (2000). In this construct, a vector containing measurements (y) is represented in terms of a forward function (F) and the combined uncertainties of this model (ε_F) and the measurement noise (ε_y) according to

$$y = F(x, b) + \varepsilon_{y,F} \ , \tag{1}$$

where F is depicted as a function of the retrieval state vector (x) (composed here of τ and r_e) and those parameters not retrieved (b) but contribute to variation in F. Assuming Gaussian error statistics, the convergent solution (iterative Newtonian) is obtained via minimization of the scalar cost function

$$\Phi = (x - x_a)^T S_a^{-1}(x - x_a) + (y - F(x, b))^T S_y^{-1}(y - F(x, b)) \tag{2}$$

which includes uncertainty covariance matrices for instrument noise and the forward model (S_y), and any a priori constraints (S_a, corresponding to x_a) made on the solution-space for the state vector.

The method is applicable to any combination of sensors, platforms, and retrieved parameters (bearing in mind the requirement of N unique equations to solve N unknowns). For these retrievals, the measurement vector was composed of GOES-10 Channels 1 and 2 (0.65 and 3.9 micron, respectively), and ACR/CDL profile information was used as a constraint on cloud height. Atmospheric profile information was obtained from rawinsonde and analyses from the European Centre for Medium-Range Weather Forecasts (ECMWF).

Case Study 1: MCSE/CAVEX in Monterey, California

The Monterey Coastal Stratus Experiment (MCSE), funded by the Office of Naval Research (ONR), studied various properties of marine stratocumulus (a persistent feature off the California coast especially during the summer months) during June-July 1999. The CloudSat Antecedent Validation Experiment (CAVEX), supported by the U.S. Department of Energy (DOE) ARM Unmanned Aerospace Vehicle (UAV) program, accompanied the MCSE. During CAVEX flights, the ACR flew aboard the DOE Twin Otter, oriented in the nadir. The stratocumulus clouds observed included both drizzle and non-drizzle conditions varying in space and time. The presence of drizzle-sized particles was inferred from the ACR by a reflectivity threshold of -15 decibels in reflectivity (dBZ) following the suggestion of Frisch et al. (1995). In situ observations were made aboard the Center for Interdisciplinary Remotely-Piloted Aircraft Studies (CIRPAS) Twin Otter using a Forward Scattering Spectrometer Probe (FSSP; Knollenberg 1976) and were collocated in time/ground-track with the DOE Twin Otter during short segments of the flights. Combined with GOES-10 retrievals along the ACR track, CAVEX provided a unique opportunity to combine in situ, cloud radar, and satellite radiometer analysis of drizzle and non-drizzle stratocumulus.

Figures 1 and 2 show the ACR backscatter profiles for 7/2/00 (drizzle) and 7/3/00 (non-drizzle), respectively, and the corresponding GOES-10 retrievals of τ and r_e are presented in Figures 3 and 4. Anomalously large effective radii retrieved for drizzle cases are demarcated in Figure 3 by a solid line at roughly 17 micrometers (μm) whereas no such anomalies were evident in the non-drizzle cases (compare against Figure 1). The forward model of the current physical retrieval assumed a simple

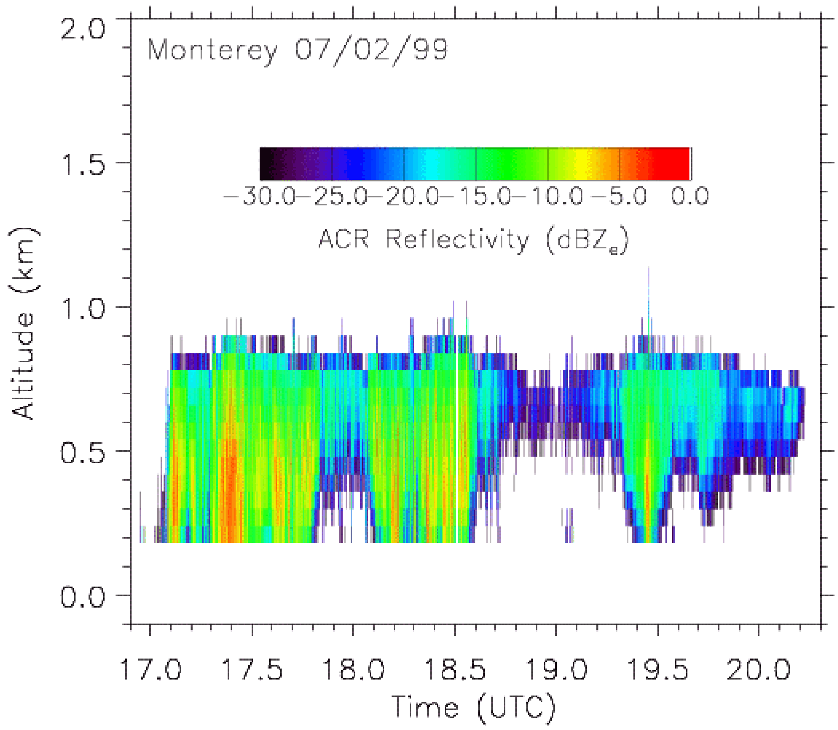

Figure 1. ACR backscatter profile of marine stratocumulus for MCSE/CAVEX drizzle case study.

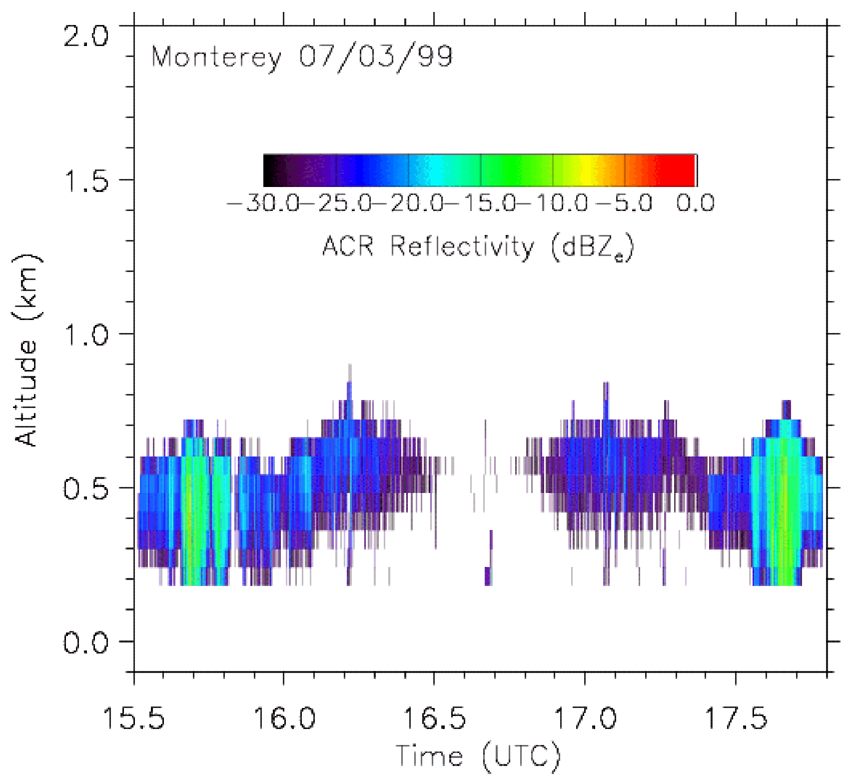

Figure 2. ACR backscatter profile of marine stratocumulus for MCSE/CAVEX non-drizzle case study.

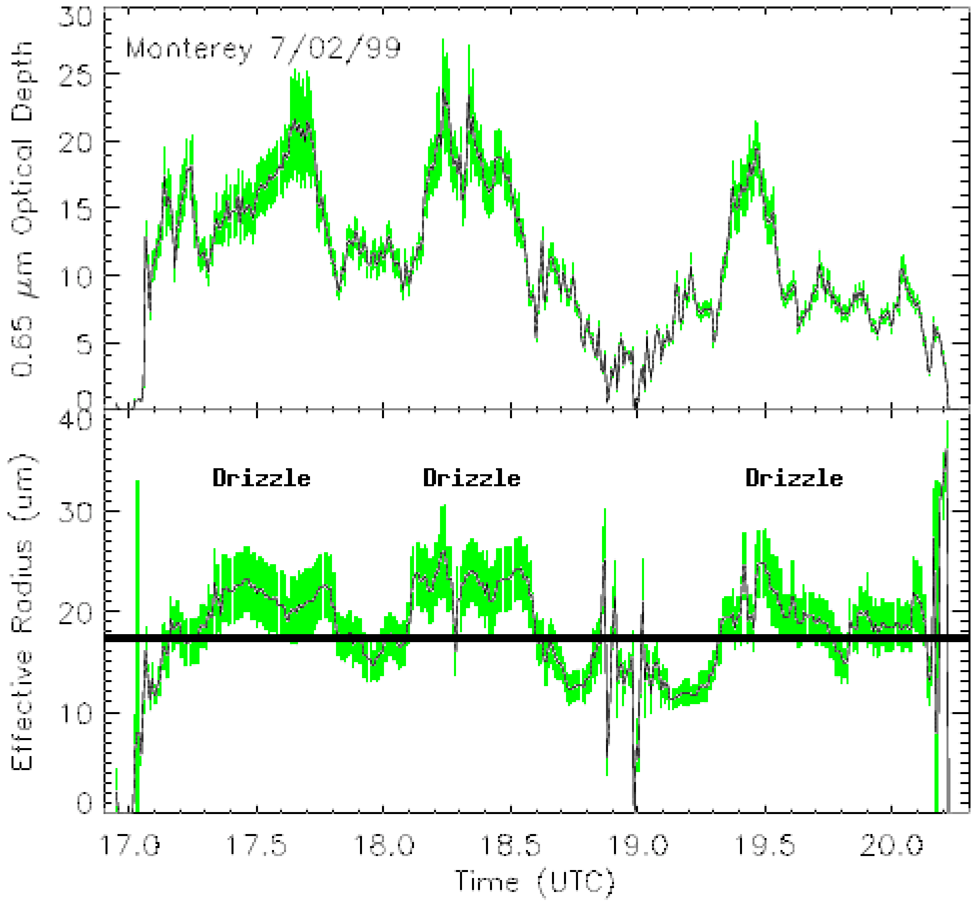

Figure 3. GOES-10 retrieval of optical depth and effective particle radius for drizzle case. Solid horizontal line corresponds to effective radius cutoff of 17 μm. "Drizzle" annotation corresponds to regions of high ACR reflectivity in Figure 1.

modified-Gamma droplet size distribution (no drizzle mode). Wiscombe et al. (1984) find that the presence of a large droplet mode in the size distribution can lead to a marked fall in shortwave cloud albedo (enhanced forward scatter of solar radiation to regions deeper within the cloud), and second and third moments are required to parameterize these effects correctly. The lower observed GOES-10 Channel 2 reflectivities owing to the presence of larger droplets are accounted for in the retrieval by adjusting r_e upward. While not representing a physical result in the context of a single-mode distribution, these large radii may prove useful as a flag for identifying potential regions of drizzle embedded within an extensive marine stratocumulus deck. The current results support previous work by Nakajima and Nakajima (1995) during the Atlantic Stratocumulus Transition Experiment (ASTEX) and are consistent with suggestions by Gerber (1996) that an r_e threshold of ~16 μm is useful for identifying regions of drizzle. The applicability to continental stratocumulus should not be implied, however, owing to significant differences in cloud microphysics in a regime of enhanced cloud condensation nuclei. Miller et al. (2000) present results from the in situ measurements for this experiment, although insensitivity of the FSSP to drizzle-sized droplets precluded their application to drizzle validation.

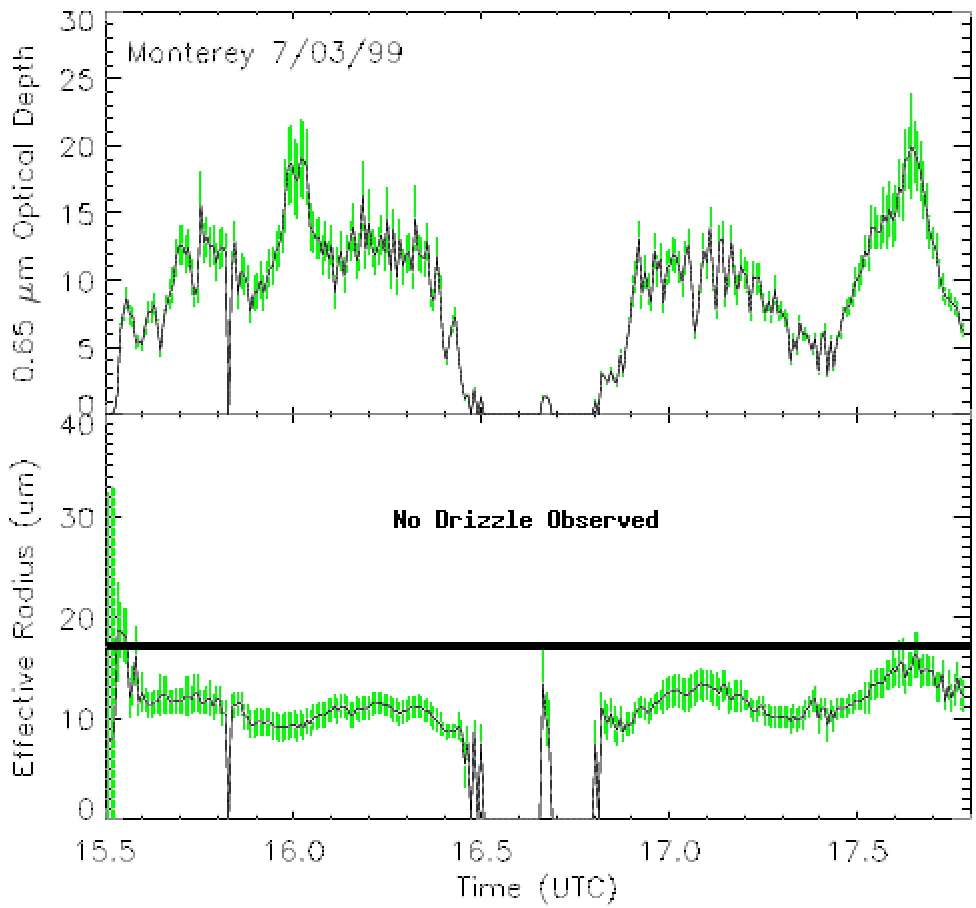

Figure 4. GOES-10 retrieval of optical depth and effective particle radius for non-drizzle case.

Case Study 2: ARM/UAV Spring Flight Series in Kauai

The ARM/UAV Spring Flight Series (SFS) was conducted during April-May 1999, and consisted of two aircraft (the Altus II UAV and the DOE Twin Otter). On April 30 the two aircraft flew in temporal/ground-track collocation while measuring tropical cirrus both from above (UAV, carrying the CDL) and below (Twin Otter, carrying the ACR). Cloud retrievals using GOES-10 imager data (and the assumption of hollow column ice crystals using the scattering phase functions of Yang and Liou [1998]) at 15-minute intervals were conducted for cases when the two aircraft were collocated within 2 minutes and 4 km. Over the course of the experiment, the layer thickened from 1.5 to 7 km with a constant cloud top near 14 km as inferred by the CDL. Rawinsonde observations revealed a deep, dry layer below 7 km that coincided closely with the cloud base as inferred by the ACR.

Figure 5 shows the active sensor observations (CDL in top panel and ACR in lower panel) for the April 30 case. The observing systems provided two very different perspectives of the same cloud field. The cloud radar was most sensitive to the large particles near the cloud base while missing (owing to a minimum detectable signal near –30 dBZ) most of the small crystals in the formation layer (producing a ragged appearance to the cloud top). In contrast, the lidar detected these smaller particles readily but the

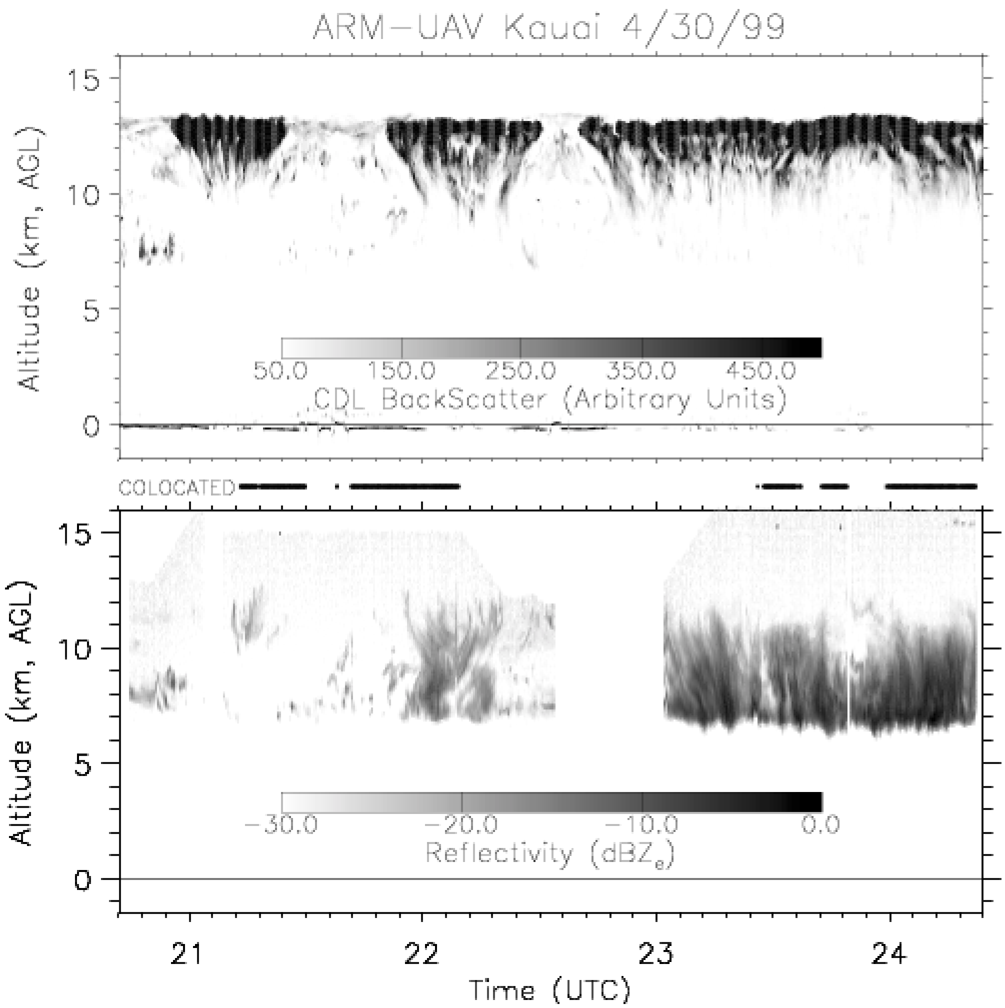

Figure 5. CDL (top) and ACR (bottom) observations of tropical cirrus during the ARM/UAV SFS on April 30, 1999. Black bars between the two panels indicate time periods where the two aircraft were collocated in ground track and time.

beam was often extinguished completely within the cloud (leaving a ragged appearance to the cloud base). Brought together, the two systems complement each other and provide information on the full cloud profile. This case study illustrates one of the primary motivations for the planned formation-flight orbits of CloudSat (carrying 94 GHz cloud radar) and Pathfinder Instruments for Cloud and Aerosol Spacebourne Observations-Climatologic Etendue des Nuages et des Aerosols (PICASSO-CENA) (carrying 532 nm lidar) satellite missions (scheduled for launch in 2003).

Shown in Figure 6 are effective radii as retrieved physically from GOES-10 and empirically from radar measurements. To estimate r_e from the ACR, ice water content (IWC, g/m^3) was first calculated using a relationship from Sassen and Liao (1996) for W-band radar

$$IWC = 0.0217 Z_i^{0.83}, \tag{3}$$

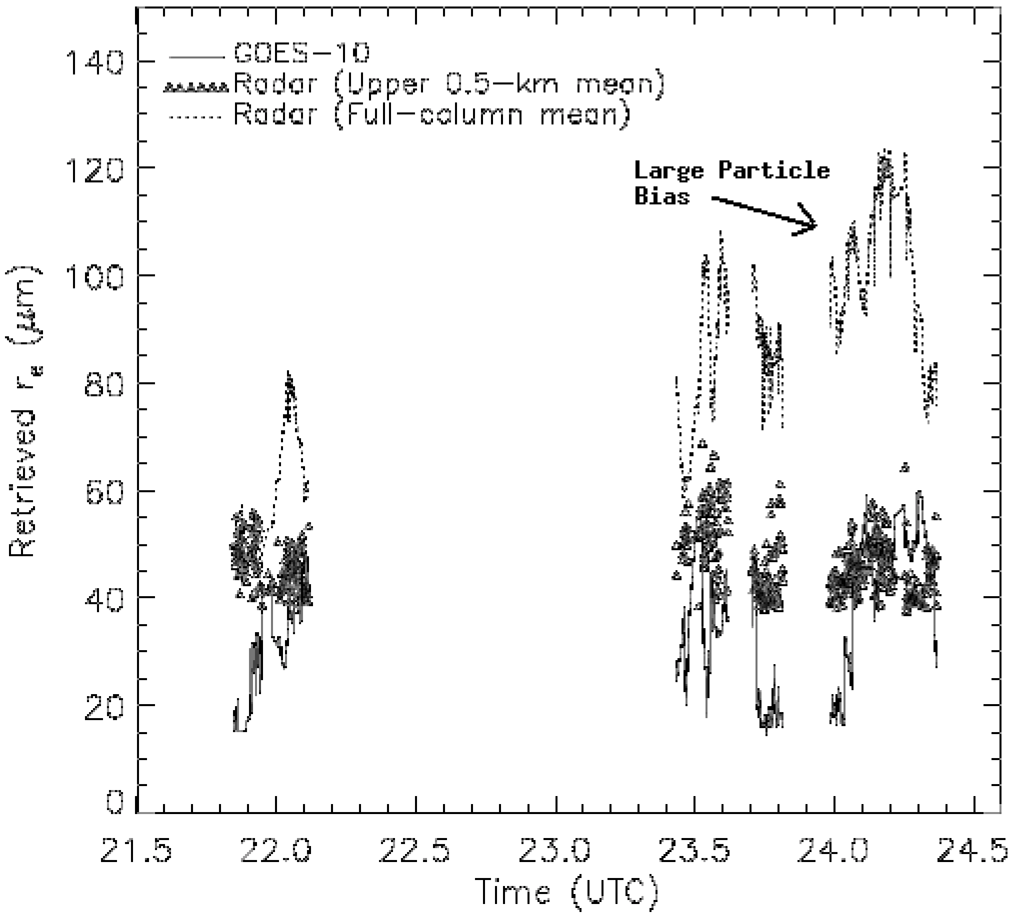

Figure 6. GOES-10 retrieved effective radius (solid), ACR retrieved column mean effective radius (dotted), and ACR retrievals adjusted to upper 0.5 km of the cloud (triangular symbols). See text for discussion.

where Z_i is the radar reflectivity (mm^6/m^3) for ice. This quantity is incorporated into a relationship between IWC and r_e developed by Platt (1997) for cirrus

$$r_e = 3IWC^{1-k} / 2j\rho \quad (4)$$

where coefficients j = 3.48 and k = 0.679 were selected for ice columns and ρ is the ice density (assumed here 0.7 g/cm^3). The radar column-mean r_e shown as a dotted line in Figure 6 includes radar range gates near the cloud base that contained values exceeding 100 μm, and was significantly larger than the GOES-10 results. When the radar results were recompiled for only the upper 0.5 km of the cloud, the adjusted r_e were observed to fall much closer to the satellite results as well as de-trend the increase in radar-computed r_e over the time period as the cloud thickened. The remaining discrepancies between GOES-10 and adjusted-radar r_e are accounted for by the lack of radar sensitivity to a large component of the upper cloud and also the empirical nature of the radar estimate itself. The sensitivity of the satellite retrievals to small cirrus crystals near cloud top and lack of sensitivity to the larger crystals near cloud base will result in a misrepresentation of cloud ice water paths inferred from passive-only systems. The radiative feedback implications of these disparities for numerical weather prediction models employing direct assimilation of satellite radiances (e.g., potential changes to the radiative heating profile affecting atmospheric stability and cloud lifetime) has not been investigated here.

Conclusion

To better understand the role of cloud radiative feedback processes in climate, next-generation observing systems capable of resolving variations in the vertical structure of their optical properties are required. Although not discussed here, cloud horizontal variability is another important factor leading to significant departures from plane parallel theory (pointing to a need for scanning active sensors). The utility of cloud radar and lidar in providing information on cloud boundaries, profiles of particle size and water content, and detection of a drizzle mode was demonstrated, and serves to place the information retrieved by passive satellite instruments in context. GOES-10 retrievals during CAVEX support claims of passive drizzle detection capability using solar reflection measurements in the visible and near infrared under certain conditions. The independent information provided by a dual active (W-band cloud radar and 1053-nm lidar) observing system is demonstrated and linked to GOES-10 observables. Namely, the effective radii retrieved by GOES-10 corresponded to the radiative properties of the upper ~0.5 to 1.0 km of the tropical cirrus examined during the ARM/UAV SFS. The complementary detection capabilities of the multi-sensor observing system provide motivation for the formation flight plan of CloudSat, PICASSO-CENA, and MODIS Aqua.

Corresponding Author

S. D. Miller, miller@nrlmry.navy.mil, (831) 656-3530

References

Frisch, A. S., C. W. Fairall, and J. B. Snider, 1995: Measurements of stratus cloud and drizzle parameters in ASTEX with a K_a-band Doppler radar and microwave radiometer. *J. Atmos. Sci.*, 52, 2788-2799.

Gerber, H., 1996: Microphysics of marine stratocumulus clouds with two drizzle modes. *J. Atmos. Sci.*, **12**, 1649-1662.

Knollenberg, R. G., 1976: Three new instruments for cloud physics measurements. Part I: Model description and sensitivity measurements, Preprints of *Int. Cloud Physics Conf.*, Boulder, Colorado, Amer. Meteor. Soc., 554-561.

Miller, S. D., G. L. Stephens, C. K. Drummond, A. K. Heidinger, and P. T. Partain, 2000: A multisensor diagnostic cloud property retrieval scheme. *J. Geophys. Res.*, **105**, 19,955-19,971.

Nakajima, T. Y., and T. Nakajima, 1995: Wide-area determination of cloud microphysical properties from NOAA AVHRR measurements for FIRE and ASTEX regions. *J. Atmos. Sci.*, **52**, 4043-4059.

Platt, C.M.R., 1997: Size spectra, extinction and ice/water content of frontal and capping cirrus clouds. *J. Atmos. Sci.*, **54**, 2083-2098.

Rodgers, C. D., 1976: Retrieval of atmospheric temperature and composition from remote measurements of thermal radiation. *Rev. Geophys.*, **14**, 609-624.

Sassen, K., and L. Liao, 1996: Estimation of cloud content by W-band radar. *J. Appl. Meteor.*, **35**, 932-938.

Wiscombe, W. J., R. M. Welch, and W. D. Hall, 1984: The effects of very large drops on cloud absorption. Part I: Parcel models. *J. Atmos. Sci.*, **41**, 1336-1355.

Yang, P., and K.-N. Liou, 1998: Single-scattering properties of complex ice crystals in terrestrial Atmosphere. *Contrib. Atmos. Phys.*, **71**, 223-248.